Effect of Chlorinated Paraffin Nanoemulsion on the Microstructure and Water Repellency of Ultra-Low Density Fiberboard

Lili Cai,[a] Qilan Fu,[b] Min Niu,[a] Zhenzeng Wu,[a] and Yongqun Xie *

This work describes a water repellent ultra-low density fiberboard (ULDF) prepared by chlorinated paraffin nanoemulsion (CPNE). Compared with the untreated ULDF, the contact angle of ULDF treated with 150 mL of CPNE increased from 40° to 134°, while its apparent surface free energy decreased from 24.19 mN/m to 10.06 mN/m. Moreover, the water absorbance of ULDF treated with CPNE decreased from 88.2% to 24% in the first hour. The improved hydrophobicity and hygroscopicity of ULDF was supported by the presence of a film on the surface of fibers, as observed by environmental scanning electron microscopy. The occurrence of chlorine and the chemical structure changes in ULDF before and after CPNE treatment were also confirmed by X-ray photoelectron spectroscopy analysis and Fourier transform infrared spectroscopy respectively. This ULDF with enhanced water repellency is a promising insulation material.

Keywords: Hydrophobic; Foam material; Chlorinated paraffin nanoemulsion; Insulation material

*Contact information: a: Department of Material Science and Engineering, Fujian Agriculture and Forestry University, 350002, Fuzhou, Fujian, China; b: Wood Research Center, Laval University, 2425, Quebec, Canada; *Corresponding author: fjxieyq@hotmail.com*

INTRODUCTION

The problems of environmental pollution and exhaustion of energy resources are becoming increasingly detrimental, and exploring and using alternative energy sources is vital (Mohanty *et al*. 2002). It is imperative to make full use of natural plant fiber and to develop renewable and biodegradable materials. Ultra-low density fiberboard (ULDF) is an environmentally friendly material mostly composed of natural fibers, and it can be obtained by a liquid foaming method (Xie *et al*. 2004, 2011). It has an ultra-low density falling between 10 and 90 kg/m^3. ULDF is favorable for noise reduction (noise reduction coefficient of 0.61 to 0.73), thermal insulation (0.02 to 0.038 W·m/K), and flame retardance (limiting oxygen index of 32) (Cai *et al*. 2014; Niu *et al*. 2014, 2015a, b). It can also be used as cushioning in packaging and low-density wall and insulation materials. However, the main raw material of ULDF is plant fiber; abundant hydroxyl groups in the cellulose molecules cause hydrophilicity (like high moisture absorption) and low resistance to water (Young 1994). The hydrophilicity of plant fibers affects the mechanical properties and durability of fiber-based composites. Therefore, improvement of water repellency of fiber is important for practical application of ULDFs.

Techniques that reduce the hydrophilicity of fiber materials include chemical modification (Mitchell *et al.* 2005; Dankovich and Hsieh 2007; Devi and Maji 2012), compositing with hydrophobic polymers (Yang *et al.* 2012), inorganic fillers (Chen *et al.* 2010), and plasma treatment (Poaty *et al.* 2013). However, chemical modification usually

consumes a lot of energy. Inorganic fillers or plasma treatment decreases the mechanical properties of biomaterials (Azambre *et al.* 2000). Compositing with hydrophobic polymers such as paraffin exacerbates the ignitability of plant fibers (Wang *et al.* 2015). Hence, a substitute for paraffin that is both incombustible and hydrophobic is necessary.

Chlorinated paraffin (CP) and chlorinated derivatives of paraffin hydrocarbon are not only feasible for industrialization and fire resistance (Camino and Costa 1980; Kind and Hull 2012) but also high water repellency (Okada *et al*. 2015; Wantling *et al*. 2015). Additionally, nanoemulsions can serve as useful performance enhancers for polymer materials because of their small size, high surface energy, and unsaturated chemical bonds on the surface (Chaudhuri and Paria 2011). Therefore, chlorinated paraffin nanoemulsion (CPNE) prepared through inversed phase emulsification of CP and emulsifier can likely be used to improve the water repellency of ULDF. When the particle size of CPNE is smaller than that of the nano-pores of fibers (Lu and Zhao 2008), the interaction between fibers and CPNE may be totally different from that between fibers and the chlorinated paraffin-70 (CP70) or chlorinated paraffin-52 (CP52) of normal size. This physical combination or chemical change may further affect the water repellency of ULDF.

However, little information has been reported on the effect of water repellency of ULDF. Unlike most recent studies focusing on the fire retardance of CP in polymers (Hornsby *et al.* 1991; Wang *et al.* 2005; Zhang *et al.* 2010), this paper investigated the effect of previously prepared CPNE on the microstructure and water repellency of ULDF. The morphological structure was analyzed to show interactions between the fibers and CPNE, and chemical composition changes were determined to support the water repellency improvement of ULDF by CPNE. Contact angle, surface tension, and hygroscopicity of the ULDF were examined to confirm the positive effect of adding the chlorinated paraffin nanoemulsion into the adhesive system.

EXPERIMENTAL

Materials

Kraft pulp (KP; consisting of spruce, pine, and fir) purchased from Tembec Inc. (Quebec, Canada) was used as the main raw material to manufacture the ULDF. CP70 and CP52 purchased from Jiangyin Saiwei Technology Trade Co. Ltd (Jiangshu, China) were used to prepare the chlorinated paraffin nanoemulsion. Alkyl phenol polyoxyethylene ether (APEO) and alcohol-polyoxyethylene ether (AEO) purchased from Tianjin Fuchen Chemical Reagents Factory (Tianjin, China) were used as emulsifiers during the preparation of CPNE.

Methods

Preparation of chlorinated paraffin nanoemulsion

CPNE was prepared by inversed phase emulsification in a triangle flask at 95 °C (oil bath pan) for 60 min using the emulsifier (mass ratio of APEO: AEO at 3:2, dosage of 18.5 wt%) to emulsify the mixture of CP70 and CP52 (mass ratio of CP70: CP52 at 2:1). The mixture was stirred at a speed of 240 rpm. To prevent coagulation, the reaction was quenched by adding 0 °C distilled water until a phase transition occurred.

Preparation of ultra-low density fiberboards

ULDFs with a target bulk density of 50 to 90 kg/m^3 were fabricated. The fabrication process of the panels is shown in Fig. 1.

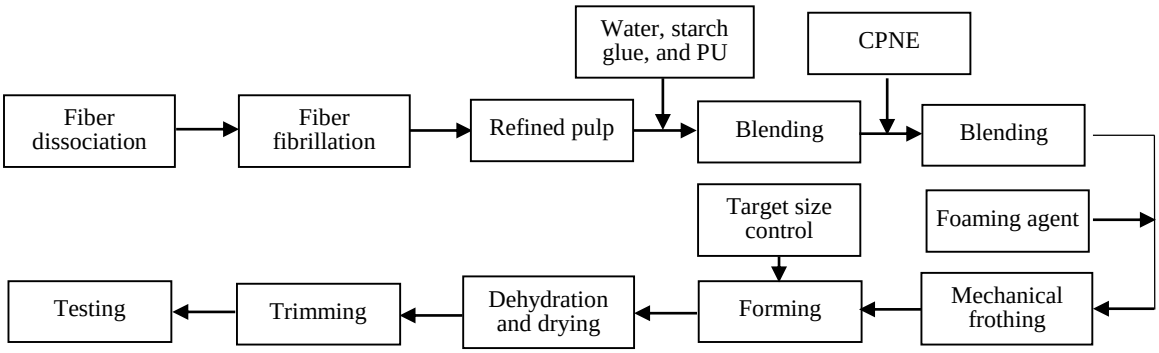

Fig. 1. The preparation of ultra-low density fiberboards

Specifically, 40 g of absolute dried mechanical pulp and 1000 mL of water were mixed in a fiber dissociator (GBJ-A, Changchun Yongxing Test Instrument Factory, Changchun, China) for 5 min. Then, 50 mL of starch glue and 10 mL of commercial polyurethane resin (PU) were added into the fiber dissociator and stirred for another 5 min to make a uniform mix. CPNE (0, 60, 90, 120, or 150 mL) and sodium dodecylbenzene sulfonate surfactant (10 wt%, foaming agent) were added into the system and allowed to foam for 3 min. Finally, the prepared sample was poured into a cubic mold of 200 mm × 200 mm × 50 mm ($L \times W \times H$) for dehydrating. The mold was dried in an electrically heated drying oven (DHG-9420A, Tianjin Experimental Instrument Factory, China) at 103 °C until the mixture reached a constant moisture content (last about 8 h).

Particle size of chlorinated paraffin nanoemulsion

The distribution of particle sizes in the dispersion was determined by a laser particle size analyzer (BT-9300H, Bettersize Instruments Ltd., Dandong, China) at a refraction coefficient of 1.33 and a scattering angle of 90°. A droplet of the CPNE was diluted in 20 mL water to measure the distribution of particle size.

Morphology of ultra-low density fiberboards

An environment scanning electron microscope (ESEM, XL30, FEI Company, USA) was used to investigate the surface morphology of ULDFs. The absolute dried sample was affixed onto the specimen holder and gold-platted operating at 10.0 kV.

Chemical changes of ultra-low density fiberboards

X-ray photoelectron spectroscopy (XPS; ESCALAB 250, ThermoFisher Scientific Inc., Waltham, MA, USA) was employed to study the surface chemical changes of ULDFs. The materials were irradiated with Al K X-rays using spot size with a diameter of 500 μm at 150 W. Spectra were recorded with pass energy of 30 eV and energy step size of 0.050 eV. XPS spectra deconvolution was conducted by OriginPro. 9.0 (Trail version, OriginLab, Hampton, Massachusetts, USA).

Fourier transform infrared (FTIR) spectra were recorded on a Nicolet 380 spectrometer (ThermoFisher Scientific Inc.). The samples were prepared by the squash

technique at a ratio of sample to KBr at 1:100 within the wavelength range of 4,000 to 400 cm^{-1} at ambient temperature.

Water repellency of ultra-low density fiberboards

Images of the water repellency experiments were recorded with a digital camera (Canon A2200, Tokyo, Japan). The photos were taken 10 min after dripping water droplets uniformly on the surface of each sample.

Sessile drop contact angle/interfacial tension measurement was performed with a JC2000A apparatus (Powereach Co. Ltd., Shanghai, China) to detect the contact angle and the surface energy of ULDFs. The absolute dried sample and KBr powder were uniformly mixed at a mass ratio of 1:100 by the tablet pressing technique. The contact angle between the tablet and water was tested, and the surface tension was recorded.

Hygroscopic property of ultra-low density fiberboards

The hygroscopic properties of ULDFs were tested by calculating the weight increase during water uptake (W_i) according to the following equation,

$$W_i\ (\%) = (W_n - W_0) / W_0 \times 100 \quad (1)$$

where W_0 is the weight of the absolute dried sample, and W_n (n = 1, 2, 3, 4, and 5) values were measured at 1 h, 2 h, 3 h, 4 h, and 5 h, respectively, after dripping 5 g of water evenly on the surface of ULDFs. The reported results were the average of five replicates.

RESULTS AND DISCUSSION

Distribution of CPNE on the Surface of ULDFs

Particle size of CPNE

The particle size of CPNE may have a direct effect on the distribution of ULDFs. The detailed particle size distribution is shown in Fig. 2, which indicated that 93.42% of the particles had a diameter size from 100 to 290 nm. Thus, the total volume of the particles larger than 290 nm was lower than 6.58% of the total volume percentage.

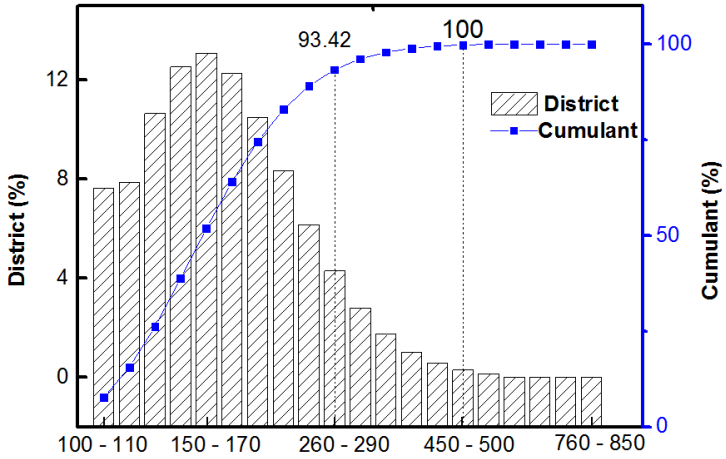

Fig. 2. The size distribution of CPNE

Also, the average median diameter and average volume mean diameter were 160 nm and 180 nm, respectively. These dimensions allowed the relatively uniform distribution of the CPNE particles as they entered into the nano-pores of the pulp fibers or cell cavities or were deposited on the fiber surface. (Zhao 2002).

ESEM micrographs on ULDFs with different content of CPNE

To investigate the distribution of CPNE on the fiber surface, the microstructure of ULDFs was investigated in further detail by ESEM (Fig. 3). Significant differences were observed between the untreated and treated samples. As expected, the surface of untreated ULDF (Fig. 3a) was very smooth and porous, which was no longer the case when the fibers were treated with CPNE. All treated fibers appeared homogeneously covered by a thin coating on their surface. Larger additions of CPNE produced thicker films covering the surface of fibers and a more wrinkled appearance. This effect may be due to the melting point of chlorinated paraffin at approximately 90 °C (Feldman 1951). The chlorinated paraffin nanoemulsion particles present on the fiber surface may melt, spread, and disappear during ULDF drying, resulting in a crinkled and irregular surface that is different from untreated ULDF. Apparently, the addition of more CPNE facilitated a more even distribution of the film and increased the roughness of fibers' surfaces due to the coverage of CPNE particles. This may be related to the water repellency of ULDF as evidence in some literature that the nano-scaled roughness can enhance the water resistance property (Gao and Jiang 2004; Chen *et al.* 2010). However, it is also possible that CPNE molecules present on the fiber surface partially penetrated the internal lamellar as the particles melted, which could affect the chemical structure of ULDFs.

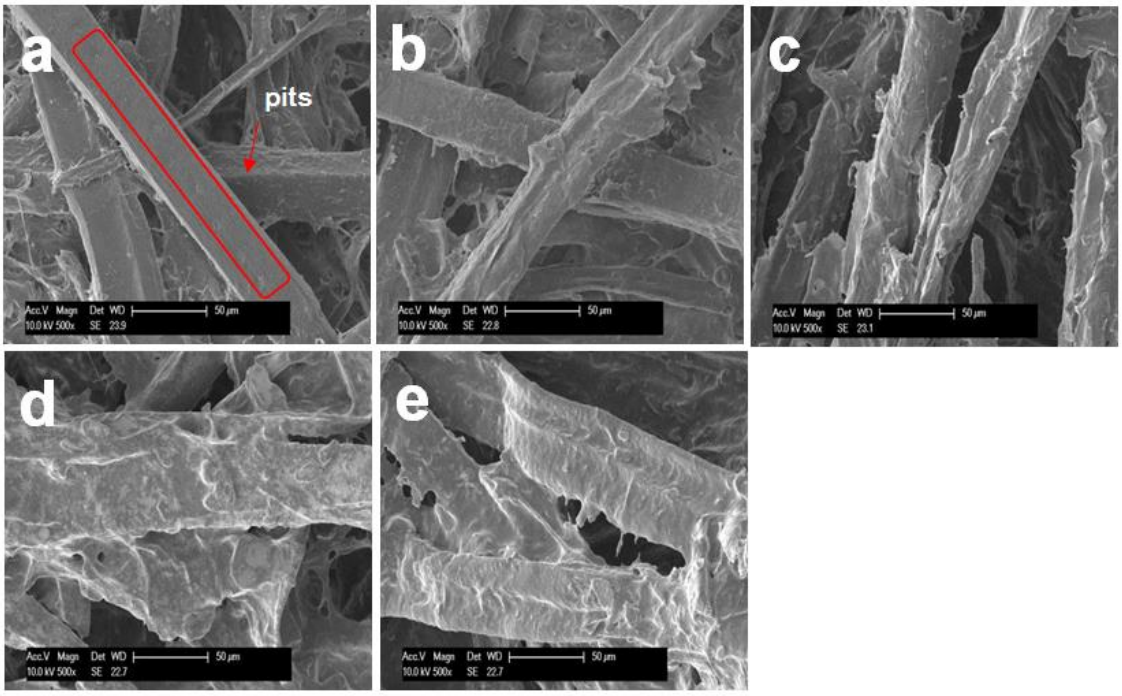

Fig. 3. Microstructure of (a) untreated ULDF and ULDFs treated with (b) 60 mL, (c) 90 mL, (d) 120 mL, or (e) 150 mL of CPNE

Chemical Bonding between CPNE and ULDFs

X-ray photoelectron spectroscopy

XPS measurements quantified the chemical composition changes in the outermost fiber surfaces of ULDFs as a function of the CPNE content. Figure 4 shows the wide scan XPS results of untreated ULDF and ULDF treated with 60 mL to 150 mL of CPNE.

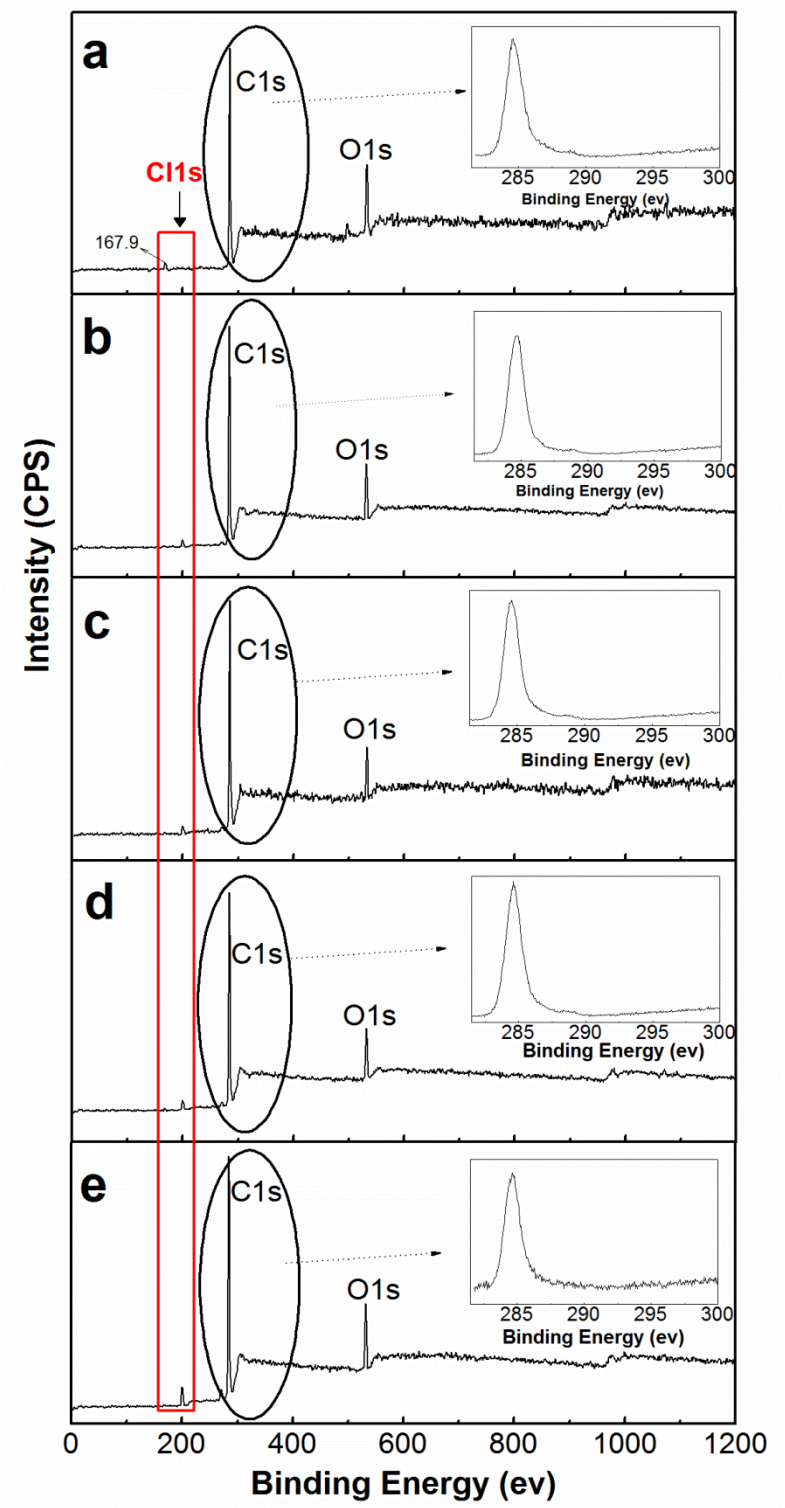

Fig. 4. XPS spectra of (a) untreated ULDF and ULDFs treated with (b) 60 mL, (c) 90 mL, (d) 120 mL, or (e) 150mL of CPNE

For all spectra, the characteristic carbon (C) and oxygen (O) peaks were present for both CPNE and ULDFs. The peak at 167.9 eV of the untreated ULDF is assigned to Si, which may stem from the raw material kraft pulp (Shea 2003). However, the chlorine peak (Cl), characteristic for the CPNE polymer, appeared only in the treated ULDF at 199.8 eV (Gauglitz and Moore 2014); together with the C1s narrow scan analysis (see insets in Fig. 4), this result confirmed the presence of CPNE on the fiber surfaces. Most importantly, the intensity of the Cl peak increased as the amount of CPNE was increased.

The insets in Fig. 4 show the C 1 peaks of both the untreated ULDF and treated ULDFs, which contained the expected three components of lignocellulose generally expressed as C 1, C 2, and C 3. For C 1, carbon atoms were bonded only to carbon and/or hydrogen atoms (C–C/C–H, around 285 eV), and C 2 refers to carbon atoms bonded to a single oxygen, forming carboxyl oxygen (C–O, about 286.5 eV). In C 3, carbon atoms were bonded to two non-carboxyl oxygen or to a single carboxyl oxygen (O–C–O or C=O, 288 to 288.5 eV) (Gauglitz and Moore 2014). The atomic concentrations of C 1 peaks and O 1s were calculated from the intensities of the bands in the spectra (Table 1).

Table 1. Atomic Concentration of C 1s, O 1s, and O/C in ULDFs

CPNE Treatment (mL)	C1 Atomic Concentration (%)	C2 Atomic Concentration (%)	C3 Atomic Concentration (%)	O Atomic Concentration (%)	O/C
0	41.7	25.2	5.8	27.3	0.38
60	45.4	22.8	4.7	27.1	0.37
90	49.4	20.8	3.1	26.8	0.36
120	51.7	21.6	2.2	24.5	0.32
150	58.6	16.4	2.2	22.7	0.29

As can be seen in Table 1, the C1 percentage increased and the C2, C3, and O/C values decreased in all treated samples. This result may reflect that CPNE contains numerous C-C and C-H bonds, so an increase in CPNE would cause the C1 content to increase. Thus, the C 2 and C 3 contents would decrease. However, the decreased C2 and C3 content, representing C-O groups or C=O groups, also revealed the presence of the CPNE on the fiber surface and the reduction of hydroxyl groups in ULDFs. The O atomic concentration of ULDFs decreased from 27.34 % to 22.69% for the untreated ULDF and ULDF treated with 150 mL of CPNE, respectively. This result confirms that a thicker film formed on the surface of fibers with the increased addition of CPNE. The O/C ratio varied between 0.38 and 0.29 for all the samples, which was also in agreement with the increased atomic concentration of C 1 and decreased atomic concentration of O 1s. The XPS results were consistent with the morphological and aggregated characteristics of ULDF from the ESEM images and the CPNE particle size distribution.

Chemical structures of CPNE and CPNE -treated ULDF

FTIR was used to confirm the chemical changes between untreated ULDF and ULDF treated with 150 mL of CPNE (Fig. 5). The spectra of both the untreated and CPNE-treated ULDF showed characteristic bands for cellulose, specifically, the OH stretching at 3500 to 3000 cm^{-1}, the CH stretching at 2915 cm^{-1}, the OH bending at 1635 cm^{-1}, the C-O stretching at 1058 and 1035 cm^{-1}, the OH out of plane bending at 623 cm^{-1}, *etc*. (Li 2003; Ferraro and Basile 2012). In particular, the untreated ULDF showed O-H stretching

vibrations at 3400 cm^{-1}, O-H stretching at 1635 cm^{-1}, and OH out of plane bending at 623cm^{-1}, which were all noticeably weakened after CPNE treatment, indicating that the surfaces of the fibers were covered with CPNE. Also, a shift of approximately 36 cm^{-1} in the -OH stretch was observed in the CPNE-treated ULDF. This shift in the hydroxyl band indicated intermolecular interaction between fibers and CPNE. In addition, the relative absorbance of the C-H bands around 2915 cm^{-1} decreased with the addition of CPNE, further confirming that the fiber surfaces were covered with CPNE. Combined with the particle size distribution and XPS data, the FTIR spectra confirmed that CPNE successfully entered into the micro/nanostructure of fibers or covered the surface of fibers in ULDF, which may have reduced the polarity of ULDF and contributed to lower surface energy.

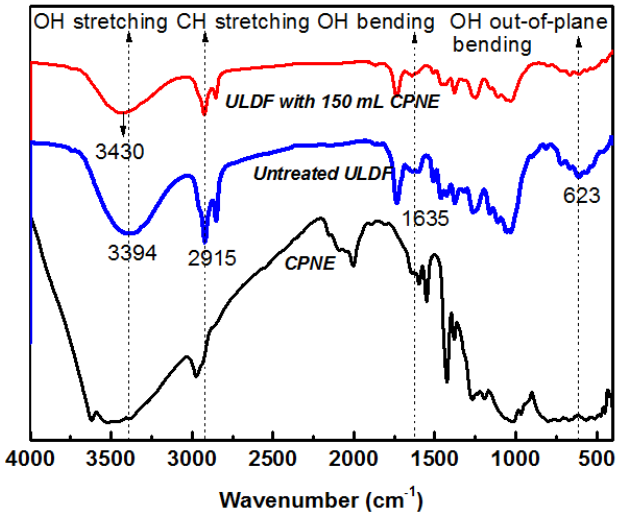

Fig. 5. FTIR spectra of CPNE, untreated ULDF, and ULDF treated with 150 mL CPNE

Water Repellency of Ultra-Low Density Fiberboards

Macroscopic views on water repellent effects of ULDFs

The beneficial effect of adding CPNE nanoparticles to the fiber-based foaming system was directly supported by improved water repellency of ULDFs (Fig. 6).

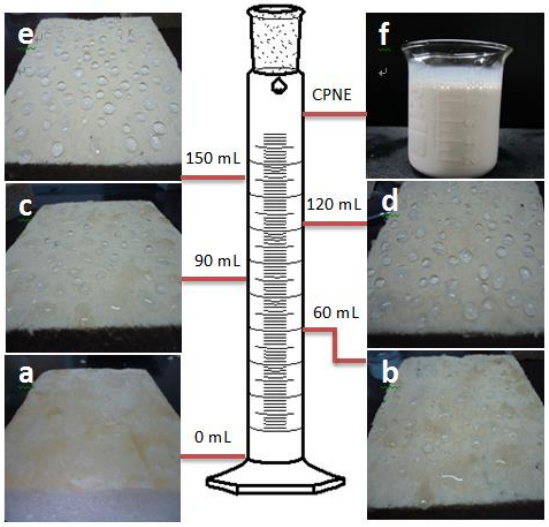

Fig. 6. Water repellency of (a) untreated ULDF and ULDFs treated with (b) 60 mL, (c) 90 mL, (d) 120 mL, or (e) 150mL of CPNE and (f) an image of CPNE

The water repellency of ULDFs increased with increasing amount of CPNE from 60 mL to 150 mL. Of all the tested samples, the untreated ULDF (Fig. 6a) demonstrated a remarkable wetting ability, while ULDF treated with 150 mL of CPNE displayed dramatically increased water repellency. Apparently, the enhanced water repellency of ULDF was attributed to the introduction of CPNE.

Contact angle of ultra-low density fiberboards

A contact angle test was used to confirm the improved water repellency of ULDFs. The scope of water contact angle θ is between 0°and 180°. When θ is below 90°, the sample is hydrophilic and *vice versa*. Photographs of a water droplet after 0.1 s of contact with each sample and the water contact angles are shown in Fig. 7. The water droplet on the surface of the untreated ULDF was almost flat, with a low contact angle of 40° (Fig. 7a), indicating that most of the water droplet was absorbed into the panel; the untreated ULDF was obviously hydrophilic. After the introduction of CPNE into the foaming system, the contact angle of ULDF was increased from 105° to 134° as a function of CPNE content. With the addition of 150 mL of CPNE, the water droplet on the surface of ULDF was approximately circular, suggesting excellent water repellency. It can also indicate that the distribution of CPNE film on the surface of ULDF may have sealed parts of the hydrogen groups of cellulose and decreased the surface tension of ULDFs.

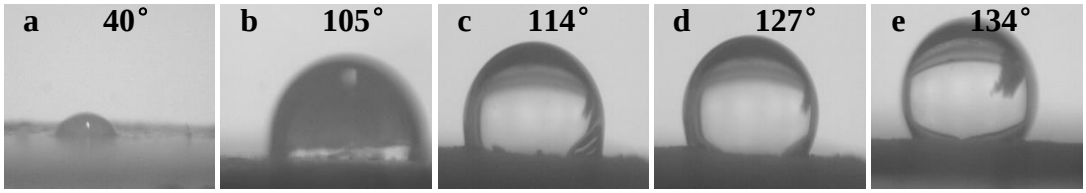

Fig. 7. The contact angles of a water droplet on (a) untreated ULDF and ULDFs treated with (b) 60 mL, (c) 90 mL, (d) 120 mL, or (e) 150 mL of CPNE

Surface tension of ULDFs

Surface tension was an important factor during water uptake (Griffin 1946; Dana and Saguy 2006).

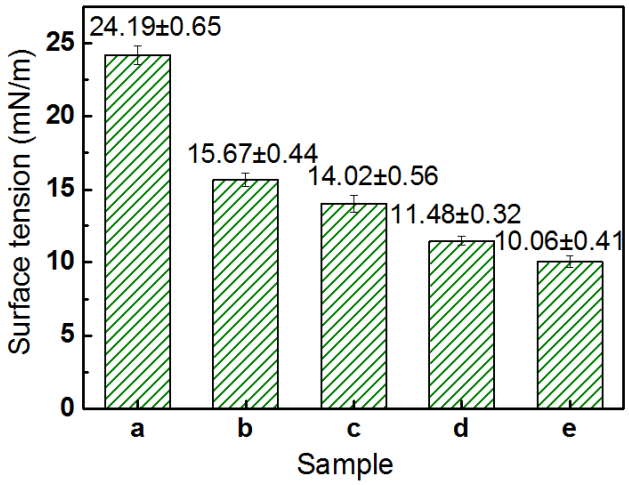

Fig. 8. Surface tensions of (a) untreated ULDF and ULDFs treated with (b) 60 mL, (c) 90 mL, (d) 120 mL, or (e) 150mL of CPNE

A higher contact angle indicates lower surface tension (Neumann *et al.* 1974). The strengthened water repellency of ULDFs was also supported by the decreased surface tension, as shown in Fig. 8.

The apparent surface energy of each sample decreased with increasing CPNE content. Compared with the untreated ULDF, the surface tension of the treated ULDFs decreased from 24.19 mN/m to 10.06 mN/m as the content of CPNE increased from 0 mL to 150 mL. Nanoparticles can approach unsaturated bonds of copolymer macromolecules and interact with the electrons of the unsaturated bonds (Friedlander 1999), resulting in a reduced surface tension. The evenly dispersed CPNE in the fiber-based material likely interact with the hydroxyl groups of the fibers (Wang *et al.* 2011). This result also confirmed that the sample was more waterproof when the material had a larger contact angle and lower surface tension. A lower surface tension facilitated a higher contact angle and enhanced the water repellency of ULDFs.

Hygroscopicity of ULDFs

The improved hygroscopicity of ULDF was also demonstrated by testing the water uptake of the CPNE-treated ULDFs (Fig. 9). The water absorption of the untreated ULDF and treated ULDFs were distinctly different. The untreated ULDF was hydrophilic and had the largest initial weight increase of 88%, which gradually decreased with time by partial evaporation of surface free water. This phenomenon was attributed to the abundant hydroxyl groups in ULDF fibers (Selvendran 1987) and the relatively large surface area of ULDF. Another possible explanation was that the velocity of water absorption was lower than that of water evaporation when the untreated ULDF became saturated.

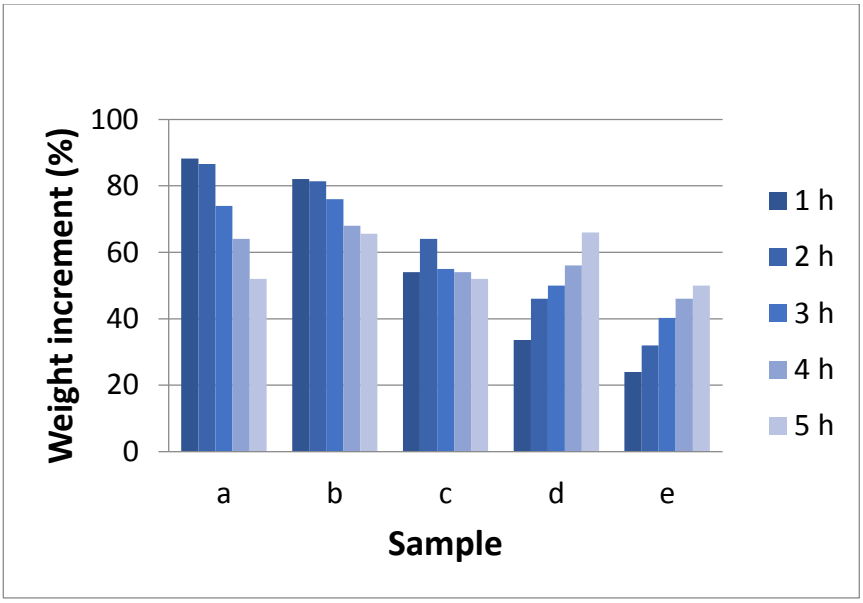

Fig. 9. Hygroscopicity of (a) untreated ULDF and ULDFs treated with (b) 60 mL, (c) 90 mL, (d) 120 mL, or (e) 150 mL of CPNE

Compared with the untreated ULDF, water absorption by the treated ULDF was clearly lower. However, a small amount of CPNE (column b, 60 mL) in ULDF did not clearly affect water uptake because of the uneven distribution of CPNE, which was in accordance with the ESEM results discussed above. In contrast, with the addition of 120

mL or 150 mL of CPNE, the water absorption of the treated ULDFs increased as a function of time. For the ULDF treated with 90 mL of CPNE, water absorption increased initially and decreased soon afterwards as a function of time. This result may be explained by the fact that the evaporated velocity of surface free water was larger than the absorbed velocity when the content of CPNE was 90 mL. Furthermore, the water absorption of ULDFs increased with decreasing CPNE content. The hydroscopicity changes caused by CPNE not only further confirmed the strengthened molecular structure of ULDFs but also supported the improved water repellency of the panels.

CONCLUSIONS

1. The chlorinated paraffin nanoemulsion (CPNE) improved the water repellency of ultra-low density fiberboard (ULDFs).
2. With the increased addition of the CPNE, the film on the fiber surface became more compact. The introduction of CPNE also modified the chemical structure of ULDF. X-ray photoelectron spectroscopy showed the presence of chlorine (Cl) in the CPNE-treated ULDF, and Fourier transform infrared spectroscopy confirmed the intermolecular interaction between fibers and CPNE.
3. Compared with the untreated ULDF, the contact angle of CPNE-treated ULDF increased, while its surface tension and water absorption decreased. Therefore, CPNE can be used to prepare a water repellent ULDF as a potential insulation material.

ACKNOWLEDGMENTS

The authors thank the Natural Science Foundation of China (NSFC) (No. 30871982) and the National Key Program of China (2008BADA9B01) for financial support.

REFERENCES CITED

Azambre, B., Heintz, O., Krzton, A., Zawadzki, J., and Weber, J. (2000). "Cellulose as a precursor of catalyst support: New aspects of thermolysis and oxidation—IR, XPS and TGA studies," *Journal of Analytical and Applied Pyrolysis* 55(1), 105-117. DOI: 10.1016/s0165-2370(99)00070-4

Cai, L. L., Xie, Y. Q., Zhuang, Q. P., and Niu, M. (2014). "Effects of polysilicate aluminum sulfate on fire resistance of ultra-low density materials," *Journal of Beijing Forestry University* 36(5), 136-141. DOI: 10.13332/j.cnki.jbfu.2014.05.002

Camino, G., and Costa, L. (1980). "Thermal degradation of a highly chlorinated paraffin used as a fire retardant additive for polymers," *Polymer Degradation and Stability* 2(1), 23-33. DOI: 10.1016/0141-3910(80)90013-0

Chaudhuri, R. G., and Paria, S. (2011). "Core/shell nanoparticles: Classes, properties, synthesis mechanisms, characterization, and applications," *Chemical Reviews* 112(4), 2373-433. DOI: 10.1021/cr100449n

Chen, X., Liu, Y., Lu, H., Yang, H., Zhou, X., and Xin, J. H. (2010). "In-situ growth of silica nanoparticles on cellulose and application of hierarchical structure in biomemetic hydrophobicity," *Cellulose* 17(6), 1103-1113. DOI: 10.1007/s10570-010-9445-3

Dana, D., and Saguy, I. S. (2006). "Review: Mechanism of oil uptake during deep-fat frying and the surfactant effect-theory and myth," *Advances in Colloid and Interface Science* 128(130), 267-272. DOI: 10.1016/j.cis.2006.11.013

Dankovich, T. A., and Hsieh, Y. L. (2007). "Surface modification of cellulose with plant triglycerides for hydrophobicity," *Cellulose* 14(5), 469-480. DOI: 10.1007/s 10570-007-9132-1

Devi, R. R., and Maji, T. K. (2012). "Chemical modification of simul wood with styrene–acrylonitrile copolymer and organically modified nanoclay," *Wood Science & Technology* 46(1-3), 299-315. DOI: 10.1007/s00226-011-0406-2

Feldman, L. V. (1951). "Chlorinated paraffin zinc containing flux," United States Patent No. 7300549A.

Ferraro, J. R., and Basile, L. J. (2012). *Fourier Transform Infrared Spectra: Applications to Chemical Systems*, Academic Press, Cambridge, MA, USA.

Friedlander, S. K. (1999). "Polymer-like behavior of inorganic nanoparticle chain aggregates," *Journal of Nanoparticle Research* 1(1), 9-15.

Gao, X. F., and Jiang, L. (2004). "Water-repellent legs of water striders," *Nature* 432(7013), 36. DOI: 10.1038/432036a

Gauglitz, G., and Moore, D. S. (2014). *Handbook of Spectroscopy* (2nd Ed.), Wiley-VCH, Weinheim, Germany.

Griffin, W. C. (1946). "Classification of surface-active agents by HLB," *Journal of Cosmetic Science* 1(3), 311-326. DOI: 10.1007/bfb0117162

Hornsby, P., Mitchell, P., and Cusack, P. (1991). "Flame retardance and smoke suppression of polychloroprene containing inorganic tin compounds," *Polymer Degradation and Stability* 32(3), 299-312. DOI: 10.1016/0141-3910(91)90003-a

Kind, D. J., and Hull, T. R. (2012). "A review of candidate fire retardants for polyisoprene," *Polymer Degradation and Stability* 97(3), 201-213. DOI: 10.1016/j.polymdegradstab.2011.12.008

Lu, W., and Zhao, G. (2008). "Structure and characterization of Chinese fir (*Cunninghamia lanceolata*) wood/MMT intercalation nanocomposite (WMNC)," *Frontiers of Forestry in China* 3(1), 121-126.

Li, J. (2003). "Wood spectroscopy," Science and Technology Press, Beijing.

Mitchell, R., Carr, C. M., Parfitt, M., Vickerman, J. C., and Jones, C. (2005). "Surface chemical analysis of raw cotton fibres and associated materials," *Cellulose* 12(6), 629-639. DOI: 10.1007/s10570-005-9000-9

Mohanty, A., Misra, M., and Drzal, L. (2002). "Sustainable bio-composites from renewable resources: Opportunities and challenges in the green materials world," *Journal of Polymers and the Environment* 10(2), 19-26. DOI: 10.1023/A:10210 13921916

Neumann, A., Good, R., Hope, C., and Sejpal, M. (1974). "An equation-of-state approach to determine surface tensions of low-energy solids from contact angles," *Journal of Colloid and Interface Science* 49(2), 291-304. DOI: 10.1016/0021-9797 (74)90365-8

Niu, M., Hagman, O., Wang, X. A., Xie, Y. Q., Karlsson, O., and Cai, L. L. (2014). "Effect of Si-Al compounds on fire properties of ultra-low density fiberboard," *BioResources* 9(2), 2415-2430. DOI: 10.15376/biores.9.2.2415-2430

Niu, M., Wang, X., Hagman, O., Karlsson, O., and Xie, Y. Q. (2015a). "Morphology of burned ultra-low density fiberboards," *BioResources* 10(4), 7292-7301. DOI: 10.15376/biores.10.4.7292-7301

Niu, M., Wang, X. A., Hagman, O., Karlsson, O., and Xie, Y. Q. (2015b). "Microstructure of burned ultra-low-density fiberboards using plant fiber as the matrix and Si-Al compounds as the filler," *BioResources* 10(2), 2903-2912. DOI: 10.15376/biores.10.2.2903-2913

Okada, T., Fujinami, Y., and Ohno, T. (2015). "Biodegradable lubricant composition," United States Patent No. 8987177.

Poaty, B., Riedl, B., Blanchet, P., Blanchard, V., and Stafford, L. (2013). "Improved water repellency of black spruce wood surfaces after treatment in carbon tetrafluoride plasmas," *Wood Science and Technology* 47(2), 411-422. DOI: 10.1007/s00226-012-0505-8

Selvendran, R. R. (1987). "Chemistry of plant cell walls and dietary fiber," *Scandinavian Journal of Gastroenterology* 129(129), 33-41. DOI: 10.3109/00 365528709095848

Shea, J. J. (2003). "Handbook of monochromatic XPS spectra - The elements and native oxides," *IEEE Electrical Insulation Magazine* 19(4), 73-73. DOI: 10.1109/mei.2003.1226740

Wang, G. J., Chen, M. H., and Liu, L. (2005). "Application of chlorinated paraffin in waterborne fire retardant coatings for steel structures," *Paint & Coatings Industry* 2(7), 31-37. DOI: 10.1016/j.surfcoat.2013.11.037

Wang, W., Zhu, Y., Cao, J., and Sun, W. (2015). "Correlation between dynamic wetting behavior and chemical components of thermally modified wood," *Applied Surface Science* 324, 332-338. DOI: 10.1016/j.apsusc.2014.10.139

Wang, Z., Gu, Z., Hong, Y., Cheng, L., and Li, Z. (2011). "Bonding strength and water resistance of starch-based wood adhesive improved by silica nanoparticles," *Carbohydrate Polymers* 86(1), 72-76. DOI: 10.1016/j.carbpol.2011.04.003

Wantling, S. J., Holder, J. L., and Wren, H. C. (2015). "Sizing and rheology agents for gypsum stucco systems for water resistant panel production," United States Patent No. 8932401.

Xie, Y., Chen, Y., and Zhang, B. (2004). "Study on a foamed material from plant fibers," *China Wood Industry* 18(2), 30-32.

Xie, Y., Tong, Q., Chen, Y., Liu, J., and Lin, M. (2011). "Manufacture and properties of ultra-low density fibreboard from wood fiber," *BioResources* 6(4), 4055-4066. DOI: 10.15376/biores.6.4.4055-4066

Yang, Q., Saito, T., and Isogai, A. (2012). "Facile fabrication of transparent cellulose films with high water repellency and gas barrier properties," *Cellulose* 19(6), 1913-1921. DOI: 10.1007/s10570-012-9790-5

Young, R. A. (1994). "Comparison of the properties of chemical cellulose pulps," *Cellulose* 1(2), 107-130. DOI: 10.1007/bf00819662

Zhang, P., Song, L., Lu, H., Wang, J., and Hu, Y. (2010). "The influence of expanded graphite on thermal properties for paraffin/high density polyethylene/chlorinated paraffin/antimony trioxide as a flame retardant phase change material," *Energy Conversion and Management* 51(12), 2733-2737. DOI: 10.1016/j.enconman.2010.06.009

Zhao, G. J. (2002). "Nano-dimensions in wood, nano-wood, wood and inorganic nano-composites," *Journal of Beijing Forestry University* 24(56), 204-207.

Article submitted: Jan. 29, 2016; Peer review completed: March 17, 2016; Revised ver. received: March 20, 2016; Accepted: March 29, 2016; Published: April 6, 2016.
DOI: 10.15376/biores.11.2.4579-4592